Protein Science (1998), 7:336–341. Cambridge University Press. Printed in the USA.

Interhelical contacts are required for the helix bundle fold of apolipophorin III and its ability to interact with lipoproteins

JIANJUN WANG,[1,2] VASANTHY NARAYANASWAMI,[1] BRIAN D. SYKES,[2] AND ROBERT O. RYAN[1]

[1]Lipid and Lipoprotein Research Group, Department of Biochemistry, University of Alberta, Edmonton, Alberta, Canada T6G 2S2
[2]Protein Engineering Networks of Centers of Excellence, Department of Biochemistry, University of Alberta, Edmonton, Alberta, Canada T6G 2S2

(RECEIVED July 16, 1997; ACCEPTED September 23, 1997)

Abstract

Apolipophorin-III (apoLp-III) from the insect, *Manduca sexta*, is a 166-residue exchangeable apolipoprotein that plays a critical role in the dynamics of plasma lipoprotein interconversions. Our previous work indicated that a 36-residue C-terminal peptide fragment, generated by cyanogen bromide digestion of apoLp-III, was unable to bind to lipid surfaces (Narayanaswami V, Kay CM, Oikawa K, Ryan RO, 1994, *Biochemistry 33*:13312–13320), and showed no secondary structure in aqueous solution. In this paper, we have performed structural studies of this peptide (E131–Q166) complexed with SDS detergent micelles, or in the presence of the helix-inducing solvent trifluoroethanol (TFE), by two-dimensional ^{1}H NMR spectroscopy. The peptide adopts an α-helical structure in the presence of both SDS and 50% TFE. The lipid-bound structure of the peptide, generated from the NMR NOE data, showed an elongated, slightly curved α-helix. Despite its high α-helix forming propensity, the peptide requires a helix-promoting environment to adopt an α-helical structure. This indicates the importance of the surrounding chemical environment and implies that, in the absence of lipid, tertiary contacts in the folded protein play a role in maintaining its structural integrity. Furthermore, the data suggest that the amphipathic helix bundle organization serves as a prerequisite structural motif for the reversible lipoprotein-binding activity of *M. sexta* apoLp-III.

Keywords: α-helix; amphipathic apolipoprotein; helix bundle; nuclear magnetic resonance

Recent advances in our understanding of the structure–function relationships of exchangeable apolipoproteins have been greatly facilitated by studies on arthropod apolipophorins. Apolipophorin III (apoLp-III) from the Sphinx moth, *Manduca sexta*, is a prototype of this class of protein, which plays a critical role in the dynamics of plasma lipoprotein interconversions. ApoLp-III is found predominantly in a lipid-free state in hemolymph, a form that is readily available to be recruited to the surface of pre-existing lipophorin particles. It is known to associate with the lipoprotein surface upon a hormone-triggered cue, during which up to 16 molecules of apoLp-III have been found to associate with a neutral lipid-loaded particle (Ryan, 1990). Clearly, there are two conformers of apoLp-III, a lipid-free and a lipid-bound form, a situation encountered frequently with other exchangeable apolipoproteins (Segrest et al., 1994). However, very little is known about the structural and mechanistic details of the interaction of exchangeable apolipoproteins with lipid surfaces.

The X-ray crystal structure of a functionally homologous apoLp-III from *Locusta migratoria* (29% sequence identity with *M. sexta* apoLp-III) shows an elongated bundle of five amphipathic α-helices (Breiter et al., 1991). The amphipathic helices are organized in such a way that their hydrophobic faces orient toward the center of the bundle, whereas their hydrophilic faces interact with the solvent. This molecular architecture resembles that of the 22-kDa N-terminal domain of human apolipoprotein E, the crystal structure of which reveals a 4-helix bundle (Wilson et al., 1991). In addition, *L. migratoria* apoLp-III is glycosylated at two Asn residues located at positions 16 and 83 (Hård et al., 1993). *M. sexta* apoLp-III, on the other hand, lacks posttranslational modifications. Also, it is monomeric and highly soluble in the absence of lipid. Thus, it serves as a good model for studying the reversible interaction between exchangeable apolipoproteins and lipoproteins.

Our previous studies suggested that *M. sexta* apoLp-III mainly adopts an α-helical structure in aqueous solution, which is enhanced upon lipid binding (Wientzek et al., 1994). Further, we demonstrated that a 36-residue peptide fragment (termed the 4K

Reprint requests to: Robert O. Ryan, Lipid and Lipoprotein Research Group, University of Alberta, Edmonton, Alberta, Canada T6G 2S2; e-mail: robert.ryan@ualberta.ca.

Abbreviations: apoLp-III, apolipophorin III; DMPC, dimyristoylphosphatidylcholine; TFE, trifluoroethanol.

peptide) of *M. sexta* apoLp-III (E131–Q166), which corresponds to the entire fifth helix and a part of the loop connecting helices 4 and 5 in the crystal structure of *L. migratoria* apoLp-III, was unstructured in aqueous solution, and was unable to bind to phospholipid vesicles or lipoprotein particles (Narayanaswami et al., 1994). Interestingly, secondary structure predictions indicate that this peptide has a high tendency to form an α-helix. Many studies indicate that the amphipathic α-helix is an essential structural element for exchangeable apolipoprotein binding to lipoprotein surfaces (see Segrest et al., 1990, 1992 for reviews). However, these studies do not completely address whether the amphipathic α-helix must pre-exist in aqueous solution, or simply possess the tendency to form an α-helix, to display lipid-binding activity. When two 9K fragments of *L. migratoria* apoLp-III were studied, both fragments were present in a random coil state in aqueous buffer and, although they could transform phospholipid bilayer vesicles into disk-like complexes, they were unable to interact with lipoprotein surfaces (Narayanaswami et al., 1995). By contrast, intact apoLp-III not only has the ability to effectively transform phospholipid vesicles into disk-like complexes (Wientzek et al., 1994), it also associates reversibly with lipoprotein surfaces (Ryan, 1996).

In this study, we have performed a two-dimensional ^{1}H-NMR study of this 36-residue peptide in three different environments, (i.e., aqueous solution, TFE, and SDS micelles). The NMR solution structure of the peptide in the presence of SDS micelles was solved using NMR NOE distance restraints. Taken together with recently obtained NMR data on the global fold of full-length lipid-free apoLp-III (Wang et al., 1997), the data suggest that interhelical contacts provide the proper environment for individual helical segments to retain their secondary structure in the absence of lipid, which is a requirement for reversible lipoprotein-binding activity.

Results and discussion

NMR assignment and secondary structure of the C-terminal 4K peptide fragment of apoLp-III

Cyanogen bromide digestion of *M. sexta* apoLp-III generated a 36-residue peptide fragment that corresponds to sequence E131–Q166 (Narayanaswami et al., 1994). Secondary structure prediction of this peptide by different algorithms in SEQSEE (Wishart et al., 1994a) suggested a high α-helix forming propensity. However, CD spectroscopy experiments indicated the peptide adopts a random coil state in aqueous solution (Narayanaswami et al., 1994). Likewise, 1D ^{1}H-NMR spectra of the amide region of the peptide in aqueous solution showed a small chemical shift dispersion that corresponded to random coil chemical shift values (data not shown). The two-dimensional NOESY spectrum in Figure 1C reveals few amide–amide proton cross peaks, confirming the predominant random coil structure of the peptide in aqueous solution. A much larger chemical shift dispersion was observed in the presence of both SDS micelles and 50% TFE, as shown in Figure 1A and B. In

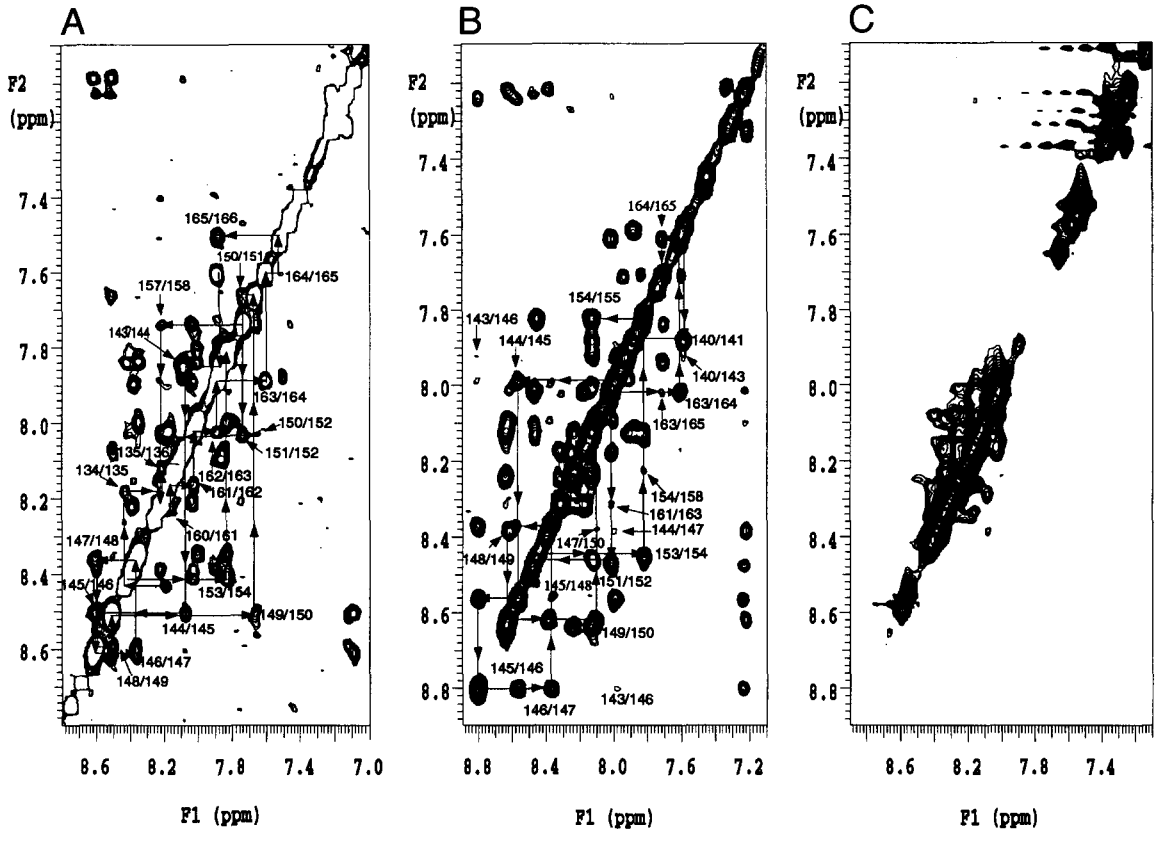

Fig. 1. Amide proton region of 2D ^{1}H-NMR NOESY spectra of *M. sexta* 4K peptide in 1% SDS micelles (**A**), 50% TFE (**B**), and aqueous solution (**C**) at pH 5.0, 25 °C with a mixing time of 300 ms. Cross peak assignments (numbered according to sequence position in intact apoLp-III) are shown by the residue numbers.

addition, many amide–amide proton cross peaks were observed, indicating an α-helical conformation of the peptide under both conditions. The spectrum in Figure 1A reveals broader cross peak line widths, suggesting slower tumbling of the peptide, consistent with peptide binding to the SDS micelles. Assignment of the NMR spectra was performed according to standard procedures as described by Wüthrich (1986), based on NOESY, TOCSY, and DQF-COSY spectra. Figure 1A and B shows some of the assignments, which include $d_{NN}(i, i + 1)$, $d_{NN}(i, i + 2)$, and $d_{NN}(i, i + 3)$ cross peaks along the peptide sequence. A summary of the NMR parameters is shown in Figure 2, including NOE connectivities, amide proton exchange rates, and chemical shift index of α-protons (Wishart et al., 1991); these indicate that the peptide adopts an α-helical conformation from L137 to K165 in the presence of SDS micelles. The first six residues showed few medium-range NOEs, indicating greater flexibility. The NMR parameters obtained in 50% TFE were similar to those in SDS micelles, except that more medium-range NOEs were observed in the first several N-terminal residues. No long-range NOEs were observed under either condition, suggesting that the peptide lacks tertiary structure in the presence of 1% SDS or 50% TFE.

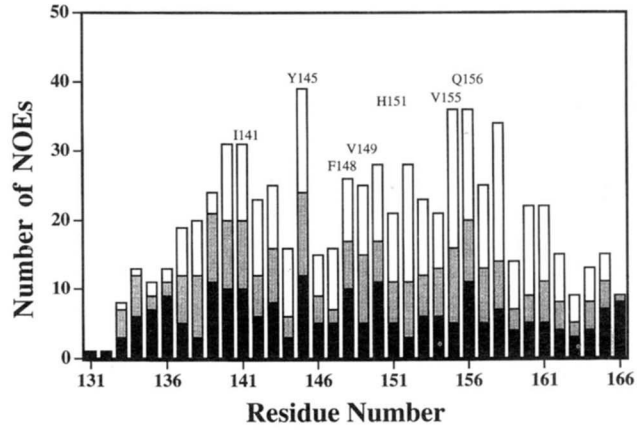

Fig. 3. Number of NOE distance restraints per residue for the 4 K peptide complexed with SDS micelles. The filled region of each bar corresponds to the number of intraresidue NOE distance restraints ($i - j = 0$), the shaded regions indicate sequential NOE distance restraints ($|i - j| = 1$), and the open regions indicate medium-range NOE distance restraints ($1 < |i - j| < 5$). Residues numbers on the x-axis or above individual bars correspond to the sequence of intact apoLp-III.

NMR structure of the 4K peptide complexed with SDS

The NMR structure of the 4K peptide was generated by a simulated-annealing protocol (Nigles et al., 1988) using the program X-PLOR (Brünger, 1992). The structure calculation was based on NOEs of the 4K peptide complexed with deuterated SDS micelles. Figure 3 shows the distribution of NOEs per residue, and indicates that the first six residues and the last residue have fewer medium-range NOEs than other residues in the peptide. However, in most cases, the overall number of NOEs per residue is larger than 10. Thus, a high-resolution NMR structure may be obtained for the 4K peptide based on the NOE data. Figure 4 shows a family of 30 NMR structures of the 4K peptide bound to SDS micelles. The structures

Fig. 2. Summary of short- and medium-range ($|i - j| \leq 3$) NOE connectivities, chemical shift index (CSI) of α-protons, and amide proton exchange rates for the 4K peptide complexed with SDS micelles. Below the one-letter code for amino acids (numbered according to the amino acid sequence of full-length apolp-III) the relative strength of $d_{\alpha N}$ and d_{NN} NOE cross peaks are indicated by the bar thickness. Various medium-range NOE connectivities between specific proton pairs are indicated by a solid line between two residues. For α-proton CSI, the negative bars indicate residues with a negative index (Wishart et al., 1991; note that a negative α-proton CSI indicates that the residue is in an α-helical region). Amide-proton exchange rate, determined as described in Materials and methods, is designated as follows: open circles, residues with medium amide proton exchange rates; closed circles, residues with slow amide proton exchange rates; no circle, fast exchange rate.

demonstrate that the first several residues in the N-terminus of the peptide are flexible, whereas it adopts an α-helical structure in the region of L137–K165. Table 1 gives the NOE violations and NMR structural statistics. A total of 469 NOEs were used for the structure calculation, among which there are 214 intraresidue, 103 sequential, and 152 medium-range NOEs (with no NOE violations > 0.3 Å). No long-range NOEs were observed, indicating a lack of tertiary contacts in the peptide structure. The final 30 NMR structures show few NOE violations, little variation from ideal covalent geometry, and low total potential energy and van der Waals energy. Table 1 also demonstrates that the NMR structures are well defined in the region of L137–K165, not only for the peptide backbone (RMSD: 0.45 Å), but also for most of the side-chain atoms in that region (RMSD: 0.97 Å). The structural data obtained for *M. sexta* apoLp-III 4K peptide are in accordance with peptide structures derived from human apolipoprotein A-I (Wang et al., 1996a) and E (Wang et al., 1996b), providing further support for the view that common functions shared by these proteins are based on their similar structural properties.

Identification of residues that bind directly to the lipid surface

Lipid association of the 4K peptide is expected to significantly reduce side-chain flexibility. The side-chain atoms of residues I141, Y145, F148, V149, H151, V155, and Q156 form a contiguous surface and are more well defined in the ensemble of structures shown in Figure 4 compared with those of neighboring residues. This suggests that they may be in direct contact with the SDS micellar surface. The interactions between these residues and the lipid surface restricts the mobility of their side chains, which gives rise to a larger number of NOEs, as shown in Figure 3.

Because the peptide adopts an α-helical structure in the presence of both SDS micelles and 50% TFE, the H-bonds within the helix should protect amide protons from exchanging with the solvent. However, the amide proton exchange of those residues that bind

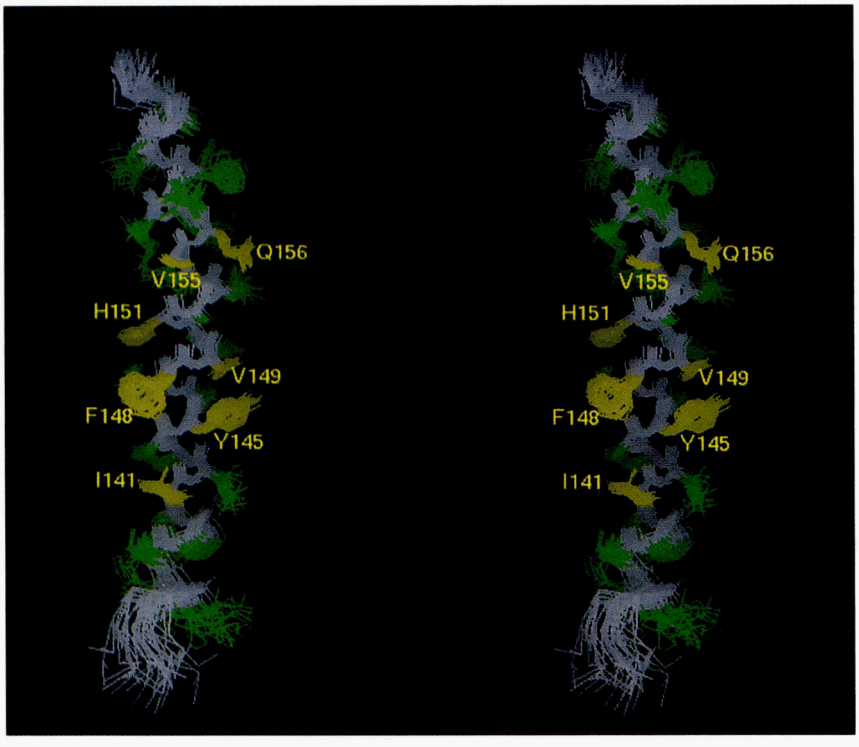

Fig. 4. Stereo view of the 4K peptide best-fit heavy atom superposition of 30 independent structures complexed with SDS. The peptide backbone is shown in gray. Residues with slow amide proton exchange rates are shown in yellow (individual residues are labeled and numbered according to the full-length apoLp-III sequence). All remaining side chains are shown in green.

directly to the lipid surface should be further protected by lipid binding. Comparison of the amide–proton exchange rates of the peptide in 50% TFE and in the presence of SDS micelles may be used as an independent method to identify residues that bind directly to the lipid surface. It was observed that the same residues with well-defined side-chain atoms (I141, Y145, F148, V149, H151, V155, and Q156) display a slower exchange rate in the presence of SDS micelles (Fig. 2) than in 50% TFE aqueous solution. On the

Table 1. *NOE violations and NMR structural statistics*

NOE violation statistics[a]	
Total NOE restraints (469) (Å)	0.017 ± 0.000
Intraresidue NOE restraints [$(i - j) = 0$] (214) (Å)	0.009 ± 0.001
Sequential NOE restraints [$(i - j) = 1$] (103) (Å)	0.022 ± 0.002
Medium-range NOE restraints [$1 < (i - j) < 5$] (152) (Å)	0.021 ± 0.004
Deviations from ideal covalent geometry	
Bonds (Å)	0.0026 ± 0.0000
Angle (deg)	0.5562 ± 0.0006
Impropers (deg)	0.3793 ± 0.0001
Energy	
E_{total} (kcal/mol)	77.64 ± 0.19
E_{NOE} (kcal/mol)[b]	7.05 ± 0.04
Structural statistics (30 structures versus the average structure)[c]	
Residue 7–33 (backbone) (Å)	0.45 ± 0.09
Residue 7–33 (heavy) (Å)	0.97 ± 0.07
Residue 7–33 (all atoms) (Å)	1.22 ± 0.07

[a]NOE violation statistics were calculated based on 30 NMR-derived solution structures of the 4K peptide.
[b]NOE force constant used in the calculations was 50 kcal/mol.
[c]Average structure is the mean atomic structure obtained by averaging the individual NMR structure following a least-squares superposition of the backbone atoms including residues 7–33.

other hand, residues such as Q143, A152, and L159 gave comparable amide exchange rates under both conditions. These results, which are consonant with the NOE data above, imply that the residues identified by a slow exchange rate when complexed with SDS micelles contact the lipid surface directly.

Interhelical contacts are critical for proper folding of M. sexta apoLp-III

Although the 4K peptide is unstructured in aqueous solution, it adopts an α-helical structure in the presence of either 50% TFE or SDS micelles. When considered together with the fact that this peptide forms the fifth helix and the preceding loop in intact apoLp-III (Wang et al., 1997), the present data suggest that micro-environment is critical for maintenance of the secondary structure of the peptide, as well as the proper global fold of the intact protein. TFE is a helix-inducing solvent, which is often used to study peptide structure (Sönnichsen et al., 1992; Wang et al., 1995), whereas SDS or dodecylphosphocholine micelles provide a model system to study the lipid-bound conformation of proteins and peptides by NMR (Wang et al., 1996a, 1996b). The smaller size of the peptide/micelle or protein/micelle complexes compared to natural lipoprotein particles results in a more rapid motion of the complex, yielding a higher-resolution NMR spectrum (Henry & Sykes, 1994). However, neither TFE nor SDS micelles accurately represent the micro-environment of helix 5 in intact lipid-free apoLp-III. The solution structure of lipid-free *M. sexta* apoLp-III (Wang et al., 1997) suggests that hydrophobic interactions between helices in the bundle provide a major force to stabilize the tertiary structure and global fold of the protein. Data obtained on the intact protein indicate extensive tertiary contacts between helix 5 and other helices in the bundle. For example, 46 interhelical NOEs were observed between helix 5 and helix 1, whereas 42 interhelical NOEs were observed between helix 5 and helix 2 (Wang et al., 1997). The observation that the 4K peptide itself is unstructured in aqueous solution, yet adopts an α-helical structure in the intact protein, and that helix 5 makes extensive contacts with the other helices, suggests that interhelical contacts are critical for stabilization of the α-helical structure of helix 5 and the proper helix-bundle fold of lipid-free apoLp-III.

Many studies suggest that an amphipathic α-helix is an essential structural element for the lipid-binding activity of exchangeable apolipoproteins (Segrest et al., 1994), and this concept is well supported by structure–function studies using synthetic peptides (Hickson-Bick at al., 1988; Sparrow et al., 1992). However, the lipid-binding assays generally used are based on relatively non-physiological, phospholipid bilayer vesicle interactions. To our knowledge, there are no reports that demonstrate binding of synthetic amphipathic α-helical peptides to spherical lipoprotein particles. Previously, we demonstrated that the 4K peptide is incapable of binding lipoprotein surfaces, and is unable to bind DMPC vesicles (Narayanaswami et al., 1994). When two larger peptide fragments (~9,000 Da), derived from *L. migratoria* apoLp-III, were characterized, they were found to interact with phospholipid vesicles and adopt a helical secondary structure, yet both were non-functional in lipoprotein binding assays (Narayanaswami et al., 1995). Finally, intact apoLp-III, which adopts a helix-bundle fold in the absence of lipid, not only has the ability to transform DMPC vesicular structures to disk-like complexes (Wientzek et al., 1994), it also effectively binds to lipoprotein surfaces (Soulages et al., 1995; Narayanaswami et al., 1996). Taken together, these results suggest a correlation between the helix-bundle structure and lipoprotein-binding activity. Thus, whereas interhelical contacts maintain the helix-bundle structure of lipid-free apoLp-III, protein–lipid interactions stabilize lipoprotein-bound apoLp-III. Subsequent alterations in lipoprotein surface properties lead to apoLp-III dissociation, which again adopts the helix-bundle structure. Thus, the helix-bundle molecular architecture in apoLp-III, and possibly other amphipathic exchangeable apolipoproteins, may serve as a structural motif to permit reversible lipoprotein-binding activity.

Materials and methods

Preparation, isolation and purification of the 4K peptide

M. sexta apoLp-III contains two Met residues, Met 12 and Met 130. Cyanogen bromide digestion generates three fragments, one of which corresponds to the C-terminal 36-residue 4K peptide. The details of the preparation, isolation, and purification of the 4K peptide have been described by Narayanaswami et al. (1994).

NMR sample preparation

Five samples were prepared for NMR studies (0.5 mL final volume in all cases). The first contained 4 mg peptide (about 2 mM) dissolved in 90% H_2O/10% D_2O at pH 5.0; the second contained 4 mg peptide dissolved in 50% TFE-d_3/50% H_2O at pH 5.0; the third contained 4 mg peptide dissolved in 90% H_2O/10% D_2O at pH 5.0, plus 1.0% SDS-d_{36}. In the third sample, the SDS:peptide concentration ratio (mol/mol) was ~60:1. The two other samples were essentially the same as samples 2 and 3, except that D_2O was used instead of H_2O. These samples were used for amide proton exchange NMR experiments.

NMR spectroscopy

All NMR experiments were performed on a Varian Unity 600 NMR spectrometer at 25 °C. The methyl signal of 2,2-dimethyl-2-silapentane-5-sulfonate was used as the chemical shift reference at 0.0 ppm. Two-dimensional DQF-COSY (Rance et al., 1983), NOESY (Jeener et al., 1979), and TOCSY (Bax & Davis, 1985) were acquired according to standard procedures. The spectral width was 6,000 Hz in both dimensions with 1,024 complex points in the t_2 dimension and 512–600 FIDs in the t_1 dimension. Typically, 32–48 scans were collected for each experiment. Presaturation was used to depress the solvent signal during both the relaxation delay and the mixing time. Two NOESY spectra were acquired, one with 300-ms mixing time (used for the assignment), the second with 150-ms mixing time (used to generate distance restraints). The TOCSY spectrum was collected with a 70-ms mixing time.

Amide-exchange experiments were performed at pH 5 using quick NOESY spectra (approximately 1 h). Only amide protons with medium and slow exchange rates were recorded. The amide proton exchange experiments were performed with a peptide/SDS sample and a peptide/TFE sample.

NMR structure generation

The NMR structure of the 4K peptide was generated using X-PLOR, version 3.1 (Brünger, 1992). Simulated annealing protocol was used for the structure calculation (Nigles et al., 1988) using NOE

distance restraints. No dihedral angle restraints were used in the structure calculation because only a few broad αH-NH cross peaks were observed in the DQF-COSY spectrum and these could not be used to obtain coupling constants. The NOE distance restraints were classified into three groups: weak, medium, and strong intensity cross peaks, which correspond to the upper boundary of the distance restraints: 5.0, 3.5, and 2.7 Å, respectively. The lower boundary of the distance restraints were set to 2.3 Å for weak cross peaks, and 1.8 Å for both medium and strong cross peaks. The distance of 2.45 Å between β-protons to the δ-proton on aromatic rings was used as a reference distance for calibration of all other NOE cross peaks. No stereospecific assignment was made during the calculation, and pseudo-atom corrections were made for protons of methylene and aromatic rings according to Wüthrich (1986). An extended structure was used as the starting structure. Structure calculation was performed using an iterative approach, in which the averaged structure of one run of calculations was used as the starting structure of the next run. Fifty structures were generated in each X-PLOR calculation. A computer program (J. Wang, manuscript in prep.) was used to automatically update the NOE restraints based on the generated structures and NOE intensities, and the new restraints were used for the next calculation until no distance restraint violations >0.3 Å were observed. The final structures were evaluated using VADAR (Wishart et al., 1994b).

Acknowledgments

This work was supported by grants from the Medical Research Council of Canada.

References

Bax A, Davis DG. 1985. MLEV-17 based two-dimensional homonuclear magnetization transfer spectroscopy *J Magn Reson 65*:355–360.

Breiter DR, Kanost MR, Benning MM, Wesenberg G, Law JH, Wells MA, Rayment I, Holden HM. 1991. Molecular structure of an apolipoprotein determined at 2.5-Å resolution. *Biochemistry 30*:603–608.

Brünger AT. 1992. *X-PLOR. A system for X-ray crystallography and NMR.* New Haven, Connecticut: Yale University Press.

Hård K, Van Doorn JM, Thomas-Oates JE, Kamerling JP, Van der Horst DJ. 1993. Structure of the Asn-linked oligosaccharides of apolipophorin III from the insect *Locusta migratoria*. Carbohydrate-linked 2-amino-ethylphosphonate as a constituent of a glycoprotein. *Biochemistry 32*:766–775.

Henry GD, Sykes BD. 1994. Methods to study membrane protein structure in solution. *Methods Enzymol 239*:515–535.

Hickson-Bick D, Knapp RD, Sparrow JT, Sparrow DA, Gotto AM Jr, Massey JB, Pownall HJ. 1988. Kinetics and mechanism of transfer of synthetic model apolipoproteins. *Biochemistry 27*:7881–7886.

Jeener J, Meier BH, Bachmann P, Ernst RR. 1979. Investigation of exchange processes by two-dimensional NMR spectroscopy *J Chem Phys 71*:4546–4553.

Narayanaswami V, Kay CM, Oikawa K, Ryan RO. 1994. Structural and binding characteristics of the carboxyl terminal fragment of apolipophorin III from *Manduca sexta*. *Biochemistry 33*:13312–13320.

Narayanaswami V, Wang J, Kay CM, Scraba DG, Ryan RO. 1996. Disulfide bond engineering to monitor conformational opening of apolipophorin III during lipid binding. *J Biol Chem 271*:26855–26862.

Narayanaswami V, Weers PMM, Bogerd J, Kooiman FP, Kay CM, Scraba DG, Van der Horst DJ, Ryan RO. 1995. Spectroscopic and lipid binding studies on the amino and carboxyl terminal fragments of *Locusta migratoria* apolipophorin III. *Biochemistry 34*:11822–11830.

Nigles M, Clore GM, Gronenborn AM. 1988. Determination of three-dimensional structures of proteins from interproton distance data by dynamical simulated annealing from a random array of atoms. *FEBS Lett 229*:129–136.

Rance M, Sorensen OW, Bodenhausen G, Wagner G, Ernst RR, Wüthrich K. 1983. Improved spectral resolution in cosy ^{1}H NMR spectra of proteins via double quantum filtering. *Biochem Biophys Res Commun 117*:479–485.

Ryan RO. 1990. Dynamics of insect lipophorin metabolism. *J Lipid Res 31*:1725–1739.

Ryan RO. 1996. Structural studies of lipoproteins and their apolipoprotein components. *Biochem Cell Biol 74*:155–174.

Segrest JP, De Loof H, Dohlman JG, Brouillette CG, Anantharamaiah GM. 1990. Amphipathic helix motif: Classes and properties. *Proteins Struct Funct Genet 8*:103–117.

Segrest JP, Garber DW, Brouillette CG, Harvey SC, Anantharamaiah GM. 1994. The amphipathic alpha helix: A multifunctional structural motif in plasma apolipoproteins. *Adv Protein Chem 45*:303–369.

Segrest JP, Jones MK, De Loof H, Brouillette CG, Venkatachalapathi YV, Anantharamaiah GM. 1992. The amphipathic helix in the exchangeable apolipoproteins: A review of secondary structure and function. *J Lipid Res 33*:141–166.

Sönnichsen FD, Van Eyk JE, Hodges RS, Sykes BD. 1992. Effect of trifluoroethanol on protein secondary structure: An NMR and CD study using a synthetic actin peptide. *Biochemistry 31*:8790–8798.

Soulages JL, Salamon Z, Wells MA, Tollin G. 1995. Low concentrations of diacylglycerol promote the binding of apolipophorin III to a phospholipid bilayer: A surface plasmon resonance spectroscopy study. *Proc Natl Acad Sci USA 92*:5650–5654.

Sparrow JT, Sparrow DA, Fernando G, Culwell AR, Kovar M, Gotto AM Jr. 1992. Apolipoprotein E: Phospholipid binding studies with synthetic peptides from the carboxyl terminus. *Biochemistry 31*:1065–1068.

Wang G, Pierens GK, Treleaven WD, Sparrow JT, Cushley RJ. 1996a. Conformations of hman apolipoprotein E(263–286) and E(267–289) in aqueous solutions of sodium dodecyl sulfate by CD and 1H-NMR. *Biochemistry 35*:10358–10366.

Wang G, Treleaven WD, Cushley RJ. 1996b. Conformation of human serum apolipoprotein A-I(166–185) in the presence of sodium dodecyl sulfate or dodecylphosphocholine by ^{1}H-NMR and CD. Evidence for specific peptide SDS interactions. *Biochim Biophys Acata 1301*:174–184.

Wang J, Gagne SM, Sykes BD, Ryan RO. 1997. Insight into lipid surface recognition and reversible conformational adaptations of an exchangeable apolipoprotein by multidimensional heteronuclear NMR techniques. *J Biol Chem 272*:17912–17921.

Wang J, Hodges RS, Sykes BD. 1995. Effect of trifluoroethanol on the solution structure and flexibility of desmopressin: A two-dimensional NMR study. *Int J Peptide Protein Res 45*:471–481.

Wientzek M, Kay CM, Oikawa K, Ryan RO. 1994. Binding of insect apolipophorin III to dimyristoylphosphatidylcholine vesicles. Evidence for a conformational change. *J Biol Chem 269*:4605–4612.

Wilson C, Wardell MR, Weisgraber KH, Mahley RW, Agard DA. 1991. Three-dimensional structure of the LDL receptor-binding domain of human apolipoprotein E. *Science 252*:1817–1822.

Wishart DS, Boyko R, Willard L, Richards FM, Sykes BD. 1994a. SEQSEE: A comprehensive program suite for protein sequence analysis. *CABIOS 10*:121–132.

Wishart DS, Sykes BD, Richards FM. 1991. Relationship between nuclear magnetic resonance chemical shift and protein secondary structure. *J Mol Biol 222*:311–333.

Wishart DS, Willard L, Richards FM, Sykes BD. 1994b. *VADAR: A comprehensive program for protein structure evaluation. Version 1.2.* Edmonton, Alberta, Canada.

Wüthrich K. 1986. *NMR of proteins and nucleic acids.* New York: John Wiley & Sons. pp 162–166.